Family of self-similar solutions of diffusion equation — Structure and Properties

Ken Sekimoto*
Matières et Systèmes Complexes, CNRS-UMR7057,
Université Paris-Diderot, 75205 Paris, France and
PCT, UMR CNRS 7083 Gulliver, ESPCI ParisTech PSL Research University, 10 rue Vauquelin, 75005 Paris, France

Takahiko Fujita†
Faculty of Science and Engineering, Department of Industrial and Systems Engineering,
Chuo University, 1-13-27, Kasuga, Bunkyo, Tokyo, Japan

The aim of the this rather technical note is to summarize the properties and utilities of the family of self-similar solutions of the diffusion equation in 1D and the similar parabolic partial-differential equations. In the first part we analyze the family of self-similar solutions focusing on the relationship among them. In the second part we describe the utility of the "exotic" self-similar solutions that decay or grow algebraically for large argument of the scaling variable.[a]

I. INTRODUCTION

When a time-evolution of physical process has no characteristic time or length, it can show the spatiotemporal self-similarity, or dynamical scaling (see Chap.10 of [1]). We mainly discuss the self-similar solutions of the one dimensional diffusion equation:

$$\frac{\partial u}{\partial t} = \frac{\partial^2 u}{\partial x^2}. \tag{1}$$

By self-similar solutions, we mean the following form,

$$u(x,t) = u_p(x,t) \equiv \frac{1}{t^{\,(p+1)/2}} \phi_p\!\left(\frac{x}{\sqrt{t}}\right), \tag{2}$$

where we call $\phi_p(s)$ the scaling function. If we substitute this form into the diffusion equation, we find that $\phi_p(s)$ should obey

$$\mathcal{L}_p\, \phi_p(s) = 0, \quad \text{with} \quad \mathcal{L}_p = \frac{d^2}{ds^2} + \frac{s}{2}\frac{d}{ds} + \frac{p+1}{2}. \tag{3}$$

The widely known solutions are the Gaussian solution with $\phi_0^{(e)}(s) = e^{-\frac{s^2}{4}}$ and the error-function solution with $\phi_{-1}^{(o)}(s) = \mathrm{erf}(s/2) \propto \int_0^s e^{-\frac{w^2}{4}} dw$, apart from the multiplicative constant, where the superfix, (e) and (o) denotes the even and odd solutions, respectively. These are well known because in most cases they are what we need about the self-similar solutions. Nevertheless, the present note will informative as background knowledge if any one of the following facts does not looks evident.

1. With $p = 0$ there is another self-similar solution, $\phi_0^{(o)}(s)$.
2. Generally the self-similar solutions (2) are not the eigenfunction of (3). p can be any real number. Therefore, there are uncountably many self-similar solutions.
3. Most of the self-similar solutions $\phi_p(s)$ has algebraic asymptots, $|s|^{-(p+1)}$ for $|s| \gg 1$ with $p \in \mathbb{R}$.
4. For non-negative integer p values, there are rapidly decaying solutions of the form $\phi_p(s) = H_p(s/2)e^{-s^2/4}$, where $H_p(z)$ is the order-p Hermite polynomial.
5. For negative integer p values, there are polynomial self-similar solutions, with the polynomial being the Hermite polynomial with imaginary argument.
6. The rapidly decaying self-similar solutions and the polynomial self-similar solutions are mutually related through the concept of integrating factor.
7. The self-similar solutions appears not only as long-time asymptote but also as short-time asymptote

In §II we discuss these points except for the last one, and the last one will be discussed in §III. In §IV we give the discussion similar to §III for other parabolic systems.

II. STRUCTURE OF THE SOLUTION FAMILY

A. Parity and general solution for all $p \in \mathbb{R}$

The operator $\mathcal{L}_p$ defined in (3) is invariant under the change $s \to -s$: That is,

$$\mathcal{L}_p \circ I = I \circ \mathcal{L}_p, \tag{4}$$

* ken.sekimoto@espci.fr, corresponding author.
† rankstatistics@gmail.com
[a] The title of Ver.1: "Exotic similarity solutions with power-law tails"

where I is the inversion operator, $I \circ \Phi(s) = \Phi(-s)$. One can, therefore, find a parameter family, $\{\phi_p(s)^{(e)}\}$, of even functions and a family, $\{\phi_p(s)^{(o)}\}$, of odd functions. The general solution can be expressed in terms of the Kummer confluent hypergeometric function, ${}_1F_1\left(a;b;z\right)$, and the Hermite polynomials, $H_p\left(z\right)$ extended to non-integer values, p [2]. The result reads

$$\phi_p(s) = e^{-\frac{s^2}{4}}\left\{{}_1F_1\left(-\frac{p}{2};\frac{1}{2};\frac{s^2}{4}\right)\phi_p(0) + \left[\frac{2^{1-p}}{p\sqrt{\pi}}\Gamma\left(\frac{2-p}{2}\right)H_p\left(\frac{s}{2}\right) - \frac{2\,\Gamma\left(\frac{2-p}{2}\right)}{p\,\Gamma\left(\frac{1-p}{2}\right)}{}_1F_1\left(-\frac{p}{2};\frac{1}{2};\frac{s^2}{4}\right)\right]\phi_p'(0)\right\}, \quad (5)$$

where the part containing of $\phi_p(0)$ and $\phi_p'(0)$ are, respectively, even and odd solutions.

B. Discrete translational symmetry in p

The operators $\{\mathcal{L}_p\}$ has the property

$$(d/ds)\mathcal{L}_p = \mathcal{L}_{p+1}(d/ds). \quad (6)$$

The consequence is that, if a solution $\phi_p(s)$ for $\mathcal{L}_p\phi_p(s) = 0$ is given for a value of p, then $\phi_{p+r}(s) \equiv d^r\phi_0(s)/ds^r$ with r being a natural number gives a solution of $\mathcal{L}_{p+r}\phi_{p+r}(s) = 0$ unless $\phi_{p+r}(s)$ is identically zero. In Fig.1 we show $\phi_{p=1}^{(o)}(s) = e^{-s^2/4}\int_0^s e^{w^2/4}dw$, and its first and second derivatives, which gives, respectively, solutions $\phi_2^{(e)}(s)$ and $\phi_3^{(o)}(s)$. We might recall that the negative values of the field are not incompatible with the positivity of the diffusion densities when the field $u_p(x,t)$ of (2) represents this field measured from some reference value, as we will do in §III B, for example.

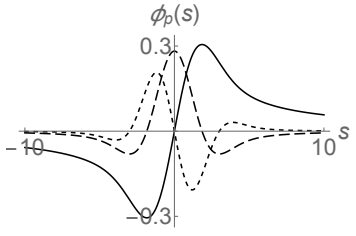

FIG. 1. Examples of the scaling functions with power-law asymptotes. Among $\phi_p(s)$ given by (5), shown are $\phi_0(s) = e^{-s^2/4}\int_0^s e^{w^2/4}dw$ (solid curve) for $p = 0$, $\phi_1(s) = \phi_0'(s)$ for $p = 1$ (dashed curve), and $\phi_2(s) = \phi_0''(s)$ for $p = 2$ (dotted curve). For $|s| \gg 1$ their amplitude decays as $\sim |s|^{-(p+1)}$ with $p = 0$, 1, and 2, respectively.

C. Algebraic asymptote and their accidental dissapearence

1. It is only when we limit the solution space to the rapidly-decaying functions that the differential equation $\mathcal{L}_p\phi_p(s) = 0$ can be regarded as an eigenvalue problem with $-(p+1)/2$ being the eigenvalue. Generically the solution $\phi_p(s)$ has algebraic asymptote, $|\phi_p(s)| \sim |s|^{-(p+1)}$ for $|s| \gg 1$. Apparently this algebraic power, $-(p+1)/2$, comes from the dominant balance between the operators $(s/2)(d/ds)$ and $(p+1)/2$ in $\mathcal{L}_p$ leaving d^2/ds^2 as less dominant. The self-similarity with power-law asymptotes has been known among the mathematicians, see, for example, [3].

2. As an immediate consequence, $|\phi_p(s)|$ with $p < -1$ diverges for $|s| \to \infty$, where $\phi_p^{(e)}$ has no zeros while $\phi_p^{(o)}$ has the only zero at $s = 0$. Except for $\phi_p^{(e)}$ with negative odd integer p and for $\phi_p^{(o)}$ with negative even integer p, the amplitude $|\phi_p(s)|$ with $p < -1$ increases rapidly with $|s|$, faster than any exponential of s.

3. For $\phi_p^{(e)}$ with negative odd integer p and for $\phi_p^{(o)}$ with negative even integer p, the scaling function $\phi_p(s)$ is polynomial, $\phi_p(s) = H_p(is/2)$ apart from the multiplicative constants. It is "accidental" due to the cancellation of the two rapidly increasing components of opposite signs.

4. Only for non-negative integer values of p, there are rapidly decaying solutions, $\phi_p(s) = H_p(s/2)e^{-s^2/4}$ apart from the multiplicative constants [3], where $H_p(s)$ is the Hermite polynomial of the s-th order. The parity of these solutions are $(-1)^p$ because of the factor $H_p(s/2)$.

5. For $p = -1$ both $\phi_{-1}^{(e)}(s) = 1$ and $\phi_{-1}^{(o)}(s) = \mathrm{erf}(s/2)$ have constant asymptots for $|s| \to \infty$.

6. As another consequence of the generic asymptote, $|\phi_p(s)| \sim |s|^{-(p+1)}$ for $|s| \gg 1$, the scaling functions $\phi_p(s)$ have algebraic tail except for $\phi_p^{(e)}(s)$ with even integer $p \geq 0$ and for $\phi_p^{(o)}(s)$ with odd integer $p \geq 1$.

7. Only for $\phi_p^{(e)}(s)$ with even $p \geq 0$ and for $\phi_p^{(o)}(s)$ with odd $p \geq 1$ the scaling function is rapidly

decaying (i.e. faster than any exponential decay) taking the above mentioned form, $\phi_p(s) = H_p(s/2)e^{-s^2/4}$. It is also "accidental" due to the cancellation of the two algebraically decaying components of opposit signs.

8. The number of nodes of $\phi_p^{(e)}(s)$ or $\phi_p^{(o)}(s)$ with $p > -1$ increases by two when the values of p is increased from below through an even integer for $\phi_p^{(e)}(s)$ or through an odd integer for $\phi_p^{(o)}(s)$, respectively. Those new zeros appear at $s = \pm\infty$.

D. Slow convergence to a self-similar solution

Note that, whether or not the scaling function is rapidly decaying, the self-similarity solutions are marginally stable in the sense that our system of interest has, by definition, no intrinsic relaxation times for the exponential decay or grow.

If the initial condition $u(x,0)$ belonging to the square integrable ($L^2(\mathbb{R})$) functional space [4], we may decompose $u(x,0)$ on the basis of the complete set, $\{H_p(x/2)e^{-x^2/4}\}_{p\in\mathbb{N}\cup\{0\}}$. The subsequent evolution by the diffusion equation is the superposition of $(t+1)^{-(p+1)/2}\ H_p(x/\sqrt{4(t+1)})\ e^{-x^2/(4(t+1))}$, for all p having non-zero components. If the mode $p_0(\geq 0)$ is the smallest non-zero component, and that p_1 the second-smallest one, the ratio between the deviation from the asymptot and the asymptot itself ($\propto (t+1)^{-(p_0+1)/2}\phi_{p_0}(x/\sqrt{4(t+1)})$) is only algebraic, $t^{-(p_1-p_0)}$.

E. Origin of rapidly decaying scaling functions

a. Adjoint operator $\mathcal{L}_p^\dagger$ — For the comprehensive understanding of the origin of these solutions we introduce the operator $\mathcal{L}_p^\dagger$ adjoint of $\mathcal{L}_p$:

$$\mathcal{L}_p^\dagger = \frac{d^2}{ds^2} - \frac{1}{2}\frac{d}{ds}s + \frac{p+1}{2}. \tag{7}$$

The adjoint differential equation $\mathcal{L}_p^\dagger\psi_p(s) = 0$ is essentially the Hermite differential equation; if we redefine $y = s/2$, the above equation becomes the standard form, $(d^2/dy^2 - 2y\,d/dy + 2p)\psi_p = 0$. In particular when p is non-negative integer, the adjoint equation has polynomial solutions, $\psi_p(s) = H_p(s/2)$, where $H_p(z)$ is the Hermite polynomial of degree $p(= 0, 1, 2, \ldots)$.

b. Integrating factor and integration by parts — Here we recall an identity equivalent to the formula of "integration by parts":

$$\begin{aligned}&\psi_p(s)\mathcal{L}_p\phi_p(s) - \phi_p(s)\mathcal{L}_p^\dagger\psi_p(s)\\ &= \frac{d}{ds}\Big[\psi_p'(s)\phi_p(s) - \psi_p(s)\phi_p'(s) - \frac{s}{2}\psi_p(s)\phi_p(s)\Big].\end{aligned} \tag{8}$$

From (8) we see that, if $\psi_p(s)$ satisfies $\mathcal{L}_p^\dagger\psi_p(s) = 0$, the term $\psi_p(s)\mathcal{L}_p\phi_p(s)$ has a primitive as shown on the right hand side. In other words, $\psi_p(s)$ serves as an integrating factor for $\mathcal{L}_p\phi_p(s) = 0$. (The dual statement also holds when we exchange ϕ_p and ψ_p.) With the knowledge of $\psi_p(s)$ the equation $\mathcal{L}_p\phi_p(s) = 0$ can be explicitly integrated: By putting $[\ldots]$ on the r.h.s. of (8) as C_2 we have

$$\phi_p(s) = C_1\,\psi_p(s)e^{-\frac{s^2}{4}} + C_2\int_{s_0}^{s}\frac{\psi_p(s)}{[\psi_p(u)]^2}e^{-\frac{s^2}{4}+\frac{u^2}{4}}du, \tag{9}$$

where C_1 and C_2 are the integration constants, and s_0 as well as the integration pathway should to be properly chosen to avoid the poles of the integrand.

Now if p is non-negative integer, we can choose as $\psi_p(s)$ the Hermite polynomial solution, $\psi_p(s) = H_p(s/2)$, and the coefficient of C_1 in (9) gives the rapidly decaying solution.

F. Relation between polynomial $\phi_p(s)$ and rapidly decaying $\phi_p(s)$

There is a further relation between $\mathcal{L}_p$ and $\mathcal{L}_p^\dagger$:

$$\mathcal{L}_p \circ J = -J \circ \mathcal{L}_q^\dagger, \qquad p + q + 1 = 0, \tag{10}$$

where we have introduced the "Wick rotation" operator J such that $J \circ \Phi(s) = \Phi(is)$ for any object including the variable s. This establishes the further relation between the solution of $\mathcal{L}_p\phi_p(s) = 0$ and that of $\mathcal{L}_q^\dagger\psi_q(s) = 0$. In particular, $\phi_p(s) = H_{-p-1}(is/2)$ satisfies $\mathcal{L}_p\phi_p(s) = 0$ for negative integers, p, because $\mathcal{L}_p^\dagger H_p(s/2) = 0$ as noted above. We, therefore, have countably many self-similarity solution which are polynomial in x of the form, $t^{m/2}H_m\big(ix/\sqrt{4t}\big)$, with $m = 0, 1, 2, \ldots$. These are related to the rapidly decaying scaling functions with non-negative integer p *via* the adjoint problem with $\mathcal{L}_p^\dagger$, as schematically represented in Fig. 2. For example, $\phi_{-3}^{(e)}(s) \propto -H_{-(-3)-1}(is/2) = s^2 + 2$ gives $u_{-3}(x,t) = x^2 + 2t$, while $\phi_2(s)^{(e)} \propto H_2(s/2)e^{-s^2/4}$.

III. MEANING AND UTILITY OF THE SOLUTIONS WITH ALGEBRAIC TAILS

A. Physical interpretation of scaling functions with algebraic asymptote

When the scaling function, $\phi_p(s)$, has an algebraic asymptote for $|s| \to \infty$, the corresponding tail in $u_p(x,t)$ is stationary in time, that is, $|u_p(x,t)| \sim$

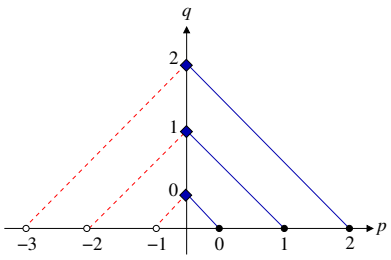

FIG. 2. Diagram showing the relations among the solutions of $\mathcal{L}_p$ and those of $\mathcal{L}_q^\dagger$. Between the pair (p,q) such that $p = q$ (for example, the solid diagonal lines), the solution of $\mathcal{L}_q^\dagger \psi_q(s) = 0$ serves as an integrating factor of the equation $\mathcal{L}_{p=q}\phi_{p=q}(s) = 0$. Between the pair (p,q) such that $p + q + 1 = 0$ (for example, the dashed diagonal lines), the solution of $\mathcal{L}_q^\dagger \psi_q(s) = 0$ gives the solution of $\mathcal{L}_{-q-1}\phi_{-q-1}(s)$ through $\phi_{-q-1}(s) = \psi_q(is)$. For $p \geq 0$ integer (thick dots) there are fast decaying solutions of the form, $\phi_p(s) = H_p(s/2)e^{-s^2/4}$. For $q \geq 0$ integer (filled diamonds) there are polynomial solutions of the adjoint problem of the form of $\psi_q(s) = H_q(s/2)$. For $p < 0$ integer (open circles) there are polynomial solutions of the form, $\phi_p(s) = H_{-p-1}(is/2)$. These three solutions are, therefore, related.

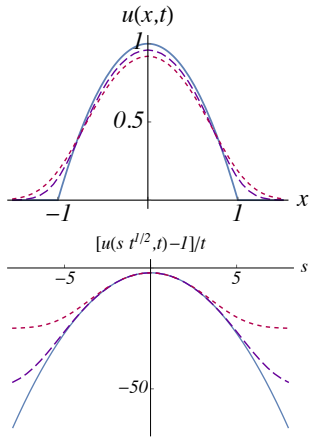

FIG. 3. Evolution of the density field in two different representations. (Left) Evolution of the density field $u(x,t)$ vs x from a truncated parabola (solid curve) drawn at $t = 0.02$ (coarse dashed curve) and 0.04 (fine dashed curve). (Right) The same results as in (Left) are represented in the scaled coordinate plane, $(u(x,t)-1)/t$ vs $s = x/\sqrt{t}$. If $-u(x,t)+1$ were self-similar, i.e. proportional to $t\phi_{-3}(x/\sqrt{t})$ with the scaling function, $\phi_{-3}(s) = 2 + s^2$, the curve should be time-independent.

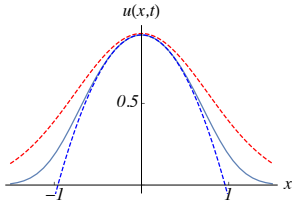

FIG. 4. Comparison between the Gaussian self-similar solution and parabolic self-similar solution. The $p = 0$ Gaussian solution, $u_G(x,t)$, is shown as the upper dashed curve, while the $p = -3$ parabolic self-similar solution, $u(x,t) - 1 = -2t - x^2$, is shown by lower dashed curve, both with regard to the true evolution (solid curve) at $t = 0.04$.

$|x|^{-(p+1)}\, t^0$ for $|x| \gg \sqrt{t}$. This stationarity is physically understandable: Because the time evolution of the diffusion system cannot modify significantly the field beyond its range of influence, $|x| \lesssim \sqrt{t}$, the only possible self-similarity outside this range is the purely spatial self-similarity, as a special case of spatio-temporal self-similarity. The purely spatial self-similarity does not imply the equilibrium: A steady diffusive flux can persist outside the range $|x| \lesssim \sqrt{t}$ and the precise form of $\phi_p(s)$ with $|s| \lesssim 1$ is determined such that it matches analytically to the stationary asymptote in the outer region, $|s| \gg 1$.

B. Short-time self-similarity around a smooth extremum

If we are to deduce the diffusion constant D from the transient evolution of the density $u(x,t)$, the self-similarity analysis around a smooth extremum is a simple approach. As an example we consider the initial distribution, $u(x,0) = \max(1 - x^2, 0)$ in a suitably chosen units (see Fig. 3(Left) solid curve). The subsequent evolution of $u(x,t)$ at $t = 0.02$ and $t = 0.04$ are numerically calculated and are also shown (Fig. 3(Left) dashed curves).

At the initial time $t = 0$, the parabolic profile is evidently the best approximation in the zone $|x| \leq 1$. We will use scaling plot, that is, after having matched the initial profile in the range $|x| \leq 1$ to the self-similarity form of $p = -3$, we draw the numerical results of $u(x,t)$ using the representation such that the self-similarity evolution remains invariant. More concretely, we compared $[u(x,t) - u(0,0)]/t$ with $-\phi_{-3}(x/\sqrt{t})$, where $\phi_{-3}(s) = 2 + s^2$. In Fig. 3(Right) we plotted $[u(x,t) - 1]/t$ vs $s = x/\sqrt{t}$ at different time, $t = 0.02, 0.04$ (dashed curves), together with the sign-inverted scaling function (solid curve). We find that the self-similarity with $p = -3$ persists near the peak while the region of "good similarity" in s narrows in time. If the purpose is to estimate the diffusion coefficient, we need the four data with dimensions, for example, $u(x_-,0), u(x_0,0), u(x_+,0)$, and $u(x_0,t_0)$ around a local maximum. The local adaptation with $u(x,t) = A[(x-B)^2 + C + 2Dt]$ will give the value of D among others.

We should note that this analysis is not equivalent to the fitting by a single Gaussian function: If we fitted the initial data $u(x,0)$ with a Gaussian function

so that the height and the peak curvature match completely, the subsequent evolution of the Gaussian function is uniquely determined by the self-similar form of $p = 0$ case, $u_0(x,t) = u_G(x,t) \equiv [\pi(1+4t)]^{-1/2} e^{-x^2/(1+4t)}$. In Fig. 4 we compare the true profiles at $t = 0.04$ (solid curve) with the Gaussian evolution thus obtained (upper dashed curve). Apparently the fitting is poorer than the parabolic self-similarity evolution (lower dashed curve). In fact the Gaussian fitting will be better adapted for the later time, when the integral conservation is important.

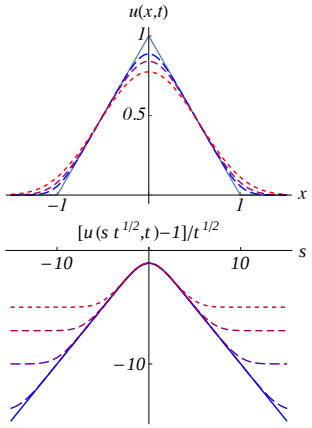

FIG. 5. Evolution of the density field in two different representations. (Left) Evolution of the density field $u(x,t)$ vs x from a truncated cusp. Initially the peak is $u(0,0) = 1$ and the support ($u(x,0) = 0$) is the zone $|x| \geq 1$. The subsequent evolution at $t = 0.005, 0.01$, and 0.02 are shown in the dashed curves with finer mesh for later time. (Right) The data at $t = 0, 005, 0.01, 0.02$, and 0.04 are represented in the scaled coordinate plane $(u(x,t) - 1)/\sqrt{t}$ vs $s = x/\sqrt{t}$. If $-u(x,t) + 1$ were self-similar, i;e., proportional to $\sqrt{t}\,\phi_{-2}(x/\sqrt{t})$ with the scaling function $\phi_{-2}(s) = e^{-s^2/4} + (\sqrt{\pi}\,s/2)\,\mathrm{erf}(s/2)$, the curve should be time-independent.

C. Self-similarity around a cusp-like extremum

When the initial field $u(x,0)$ has a cusp or wedge as function of x, its subsequent relaxation should locally obey the self-similarity form (2) with $p = -2$. The even scaling function is $\phi^{(e)}_{-2}(s) = (\sqrt{\pi}/2)\mathrm{erf}(s/2)s + e^{-s^2/4}$, corresponding to $u^{(e)}_{-2}(x,t) = (\sqrt{\pi}/2)\mathrm{erf}(x/\sqrt{4t})\,x + \sqrt{t}\,e^{-x^2/4t}$ As an example, we consider a cusp-shaped initial profile with a support: $u(x,0) = \max[1 - |x|, 0]$, see Fig. 5(Left) (solid curve). Such initial profile could be realized in the thermal conduction experiment by attaching thermostats at $x = 0$ and $x = \pm 1$ for $t < 0$. If we remove these thermostat at $t = 0$, the subsequent evolution of $u(x,t)$ obeys the diffusion equation. The spatial profiles of $u(x,t)$ are shown in the same figure, Fig. 5(Left), at $t = 0.005, 0.01$, and 0.02. We can see that a part of the initial straight slopes persist.

We made again the scaling plot as in the previous case: More concretely, we compered $[u(x,t) - u(0,0)]/\sqrt{t}$ with $-\phi_{-2}(x/\sqrt{t})$, where $\phi_{-2}(s) = e^{-s^2/4} + (\sqrt{\pi}\,s/2)\mathrm{erf}(s/2)$. In Fig. 5(Right) we plotted $[u(x,t) - 1]/\sqrt{t}$ vs $s = x/\sqrt{t}$ at different time, $t = 0.005, 0.01, 0.02, 0.04$, together with the sign-inverted scaling function (solid curve). Again we find the self-similarity holds near the rounded cusp.

IV. SIMILARITY SOLUTIONS WITH ALGEBRAIC TAILS FOR OTHER PARABOLIC DIFFERENTIAL EQUATIONSL

A. Smoothing of an initial cusp in linearized capillary-driven thin-film equation

The capillary evolution of the profile of the free surface of a thin viscous liquid film occurs as the quasi-static balance between the Laplace pressure and the viscous force due to the flow, see [7] and the references cited therein:

$$\frac{\partial u}{\partial t} = -\frac{\partial^4 u}{\partial x^4}. \tag{11}$$

If we assume the similarity form,

$$u(x,t) = t^{-\frac{\beta+1}{4}}\,\phi\left(\frac{x}{t^{\frac{1}{4}}}\right), \tag{12}$$

the scaling function $\phi(s)$ should obey

$$-\phi''''(s) + \frac{s}{4}\phi'(s) + \frac{\beta+1}{4}\phi(s) = 0. \tag{13}$$

[7] has studied the special case corresponding to $\beta = 0$ in which the solution decays rapidly in space. For generic value of β the solution $\phi(s)$ or its derivatives $\phi'(s)$ do not decay rapidly. This fourth order differen-

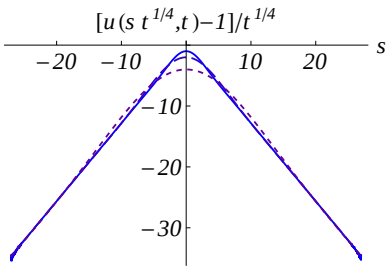

FIG. 6. Self-similar solution with algebraic asymptote of capillary-driven thin-film equation. The solution $u(x,t)$ for (11) which tends to $u(x,0) = 1 - |x|$ is shown at different moments of time, $t = 1$ (solid curve), $t = 2^4$(long dashed curve) and $t = 2^8$(short dashed curve).

tial equation has two odd solutions and two even solutions. If we fix the value of $\beta \in \mathbb{R}$, and choose the even parity, one of the two solutions can have the power-low asymptote, $\phi(s) \sim |s|^{-(\beta+1)}$, while the other solution increases very rapidly. In order to eliminate the latter component, we have to choose the ratio $\phi''(0)/\phi(0)$. Once it is done, the field $u(x,t)$ shows the static asymptote,

$$u(x,t) \sim |x|^{-(\beta+1)}, \qquad |x| \gg t^{\frac{1}{4}}. \tag{14}$$

Our interest is in the case of $\beta = -2$, which adapts to the asymptotes $u(x,t) \sim |x| + \text{const.}$ for $|x| \gg t^{1/4}$ if we choose $\phi''(0)/\phi(0) = 0.7396687797971602 + o(10^{-16})$. See Fig. 6. If the evolution equation is modified to have nonlinearity in $\phi(s)$ and more than one terms on the right hand side, the exponent corresponding to β would be fixed to discrete values. See, for example, [8] that studies the rupture of thin film due to the presence of the Van der Waals interaction.

B. Network displacement of three-dimensional gel with a power-law tail

We present here an example of the self-similarity starting from the field having a power-law tail. The system considered is an aqueous gel, or, a soft solid consisting of a very dilute polymer network saturated with water. Under an osmotic pressure gradient the water permeates through this network very slowly. By contrast, if we apply a mechanical force on the gel, its short-time response is that of an incompressible isotropic elastic body. Suppose that we prepared a uniform bulk aqueous gel having a small water-filled hole in its center with the radius R_0 around the origin, $r = 0$. At $t = 0$ we somehow increase suddenly the radius of the water-filled hole from R_0 to R_1. As the instantaneous response of the gel, the material point which has been at the radius r is displaced by the distance $U_{\rm rad}(r, 0^+)$ such that the incompressibility condition holds. For $r \gg R_1$ it reads $4\pi r^2 U_{\rm rad}(r,0^+) = (4\pi/3)[R_1^3 - R_0^3]$. The power-law asymptote $U_{\rm rad}(r,0^+) \propto r^{-2}$ for $r \gg R_1$ is thus introduced. The subsequent very slow permeation obeys the standard elasto-hydrodynamic model [9], which gives the following time evolution equation for the displacement field $U_{\rm rad}(r,t)$:

$$\left(\frac{\partial}{\partial t} - D\left[\frac{\partial^2}{\partial r^2} - \frac{2}{r^2}\right]\right)[r\, U_{\rm rad}(r,t)] = 0, \tag{15}$$

where D is the (cooperative) diffusion constant $D = (K + 4\mu/3)/f$, with f, μ, K being, respectively, the friction coefficient between the gel network and solvent, the shear modulus and bulk (osmotic) modulus of the gel [10].

Hereafter we will look at the regime with $r \gg R_1$ and $\sqrt{Dt} \gg R_1$, and will use the units such that $D = 1$. Like the diffusion equation, Eq.(15) allows the similarity solutions of the form, $U_{\rm rad}(r,t) = U_p^{(r)}(r,t) \equiv t^{-(p+1)/2}\Psi_p\big(r/\sqrt{t}\big)$. Among these solutions with different values of p, we will see that the case of $p = 1$ is compatible with the asymptote, $U_{\rm rad}(r,0) \sim r^{-2}$. Into Eq.(15) we substitute the form of the radial displacement,

$$U^{(\rm r,t)} = U_p^{(\rm r)}(r,t) \equiv \frac{1}{(Dt)^{\frac{p+1}{2}}}\Psi_p\left(\frac{r}{\sqrt{Dt}}\right).$$

We then obtain the ordinary differential equation for $\Psi_p(s)$ with $s > 0$:

$$2s^2\Psi_p''(s) + s(s^2+4)\Psi_p'(s) + ((p+1)s^2 - 4)\Psi_p(s) = 0. \tag{16}$$

In addition to the far field condition, $\Psi_p(\infty) = 0$, we impose the boundary condition at $s = 0$ which is compatible with the mostly homogeneous dilatation around the origin. In terms of the displacement vector field $\vec{U}$, this is $\vec{U}(\vec{r},t) = c(t)\,\vec{r} + \mathcal{O}(r^3)$ for $r \downarrow 0$ with $c(t)$ being a function of time. We then impose $\Psi_p(0) = 0$. Under these boundary conditions, the solutions of Eq.(16) is written in terms of the confluent hypergeometric function ${}_1F_1(a;b;z)$. The solution reads

$$\Psi_p(s) = \Psi_p'(0)\, s \times {}_1F_1\left(1 + \frac{p}{2}; \frac{5}{2}; -\frac{s^2}{2}\right). \tag{17}$$

This solution behaves as $\Psi_p(s) \simeq \Psi_p'(0)\, s$ for $0 \le s \ll 1$ and $\Psi_p(s) \sim s^{-(p+1)}$ for $s \gg 1$. Because $U_{\rm rad}(r,0) \sim r^{-2}$, we choose $p = 1$. Then we have

$$\Psi_1(s) = \Psi_1'(0) \times \frac{6}{s^2}\left[-s\, e^{-\frac{s^2}{4}} + \sqrt{\pi}\,\mathrm{erf}\left(\frac{s}{2}\right)\right]. \tag{18}$$

We show in Fig.7 the similarity solution, $U_1^{(\rm r)}(r,t) = t^{-1}\Psi_1(r/\sqrt{t})$, at $t = 1, 4$ and 9. We observe that the algebraic tail of the radial displacement at large r remains stationary until the time $t \sim r^2$. The presence of the water-filled hole would modify the radial displacements at small radius, $r \lesssim R_0$, but does not affect the fate of the algebraic tail.

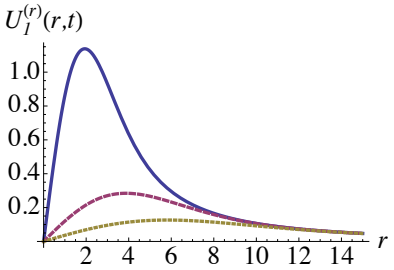

FIG. 7. Radial displacement of the gel outside a water hole. The radial displacement, $U_{\rm rad}(r,t) = U_1^{(r)}(r,t) \equiv t^{-1}\Psi_1(r/\sqrt{t})$, is shown vs r for the various time, $t = 1$(solid curve), 4 (dashed curve), and 9 (dotted curve). The vertical scale has been arbitrarily fixed. For $r \gg \sqrt{t}$ the displacement, $U_1^{(r)}(r,t)$, retains a time-independent tail, $\sim r^{-2}$.

V. CONCLUSION

The polynomial scaling functions with negative integer p are as useful as the rapidly decaying ones with non-negative integer p, and they are mutually related Going further into the general mathematical aspect of the self-similarity would require the application of the Lie group symmetry [6].

[1] J. Gunton and M. Droz, *Introduction to the theory of metastable and unstable states* (Springer-Verlag, 1983).

[2] M. Abramowitz and I. A. Stegun, *Handbook of mathematical functions with formulas, graphs, and mathematical tables*, National Bureau of Standards Applied Mathematics Series, Vol. 55 (Dover, London, 1965) pp. 505, 691.

[3] G. van Baalen, N. Popović, and C. E. Wayne, SIAM J. Math. Anal. **39**, 1951 (2007).

[4] I. C. Christov and H. A. Stone, PNAS **109**, 16012 (2012).

[5] G. I. Barenblatt, *Scaling, self-similarity, and intermediate asymptotics* (Cambridge University Press, Cambridge, 1996).

[6] G. W. Bluman and J. D. Cole, J. Math. and Mech. **18**, 1025 (1969).

[7] M. Benzaquen, T. Salez, and E. Raphaël, The European Physical Journal E **36**, 82 (2013).

[8] W. W. Zhang and J. R. Lister, Physics of Fluids **11**, 2454 (1999).

[9] T. Tanaka, L. O. Hocker, and G. B. Benedek, J. Chem. Phys. **59**, 5151 (1973).

[10] P. G. de Gennes, *Scaling Concepts in Polymer Physics* (Cornell University Press, Ithaca, NY, 1979).